Prime Numerators of the Triangular-Fractional Grid

A shell stratification and a lens for prime-in-progression density

Jeffery Huckstead
Cerebral Graphix ORCID 0009-0007-0234-2177

Draft v0.1 — July 2026

Abstract

We study the *prime numerators* of the triangular-fractional grid $a(n,k) = n - 1 + k/n$. Grouping the reduced fractions by their reduced denominator (their *shell* $s = n/\gcd(k,n)$) gives a stratification of the prime numerators that we did not find in the surveyed literature as a named object. We show that within a fixed shell the numerator has the closed form $R_s(m,t) = s^2m - s + t$, so each shell is a union of $\varphi(s)$ arithmetic progressions modulo s^2. This reduces the per-shell prime-density question to the prime-number theorem in arithmetic progressions. The naive comparison of per-shell prime density against $1/\varphi(s)$ shows a strong, persistent upward trend (Spearman $\rho_{\mathrm{Sp}} \approx 0.96$–$0.99$); this trend *vanishes* under the cellwise predictor $\widehat{\rho}_N(s)$, whose coprimality factor $s/\varphi(s)$ is exact because $\varphi(s^2) = s\varphi(s)$. The corrected ratio is flat with no trend, its coefficient of variation *shrinks* with N ($0.138 \to 0.058$ across $N = 250 \to 2000$), and at $N = 1000$ a fraction 0.994 of shells fall within two binomial standard errors of the prediction. We conclude that the shell stratification is a **lens, not a new prime law**: the triangular-fractional shell coordinate makes a classical prime-in-progression mechanism visible in a clean, controlled way. We prove a within-shell numerator-uniqueness result, record the controls, and fence the claim explicitly. No new prime phenomenon, no Riemann-hypothesis relevance, and no higher-dimensional claim is asserted.

1 Introduction and scope

The triangular-fractional grid places, in chamber $n \geq 1$, the n rational points

$$a(n,k) = n - 1 + \frac{k}{n} = \frac{n(n-1)+k}{n}, \qquad 1 \leq k \leq n.$$

The parent paper establishes the exact divisor-band structure: a reduced fraction r/s occurs in chamber n precisely when $s \mid n$ and $s(n-1) < r \leq sn$, so each divisor $s \mid n$ contributes $\varphi(s)$ reduced entries. The Jordan Chamber Lift companion extends the denominator-shell bookkeeping to d Cartesian dimensions ($\sum_{q|n} J_d(q) = n^d$) and separates the finite shell density $J_d(q)/q^d$ from the visible-lattice density $1/\zeta(d)$.

Both prior works study the *fractions* and their *denominators*. This note studies the *numerators*, and specifically **which reduced numerators are prime**, organized by shell. We treat this as a lens: a way to organize the prime numerators so that a classical mechanism becomes visible. The contribution is the triangular-fractional-native organization and the controlled demonstration; the underlying arithmetic, once unfolded, is the prime-number theorem in arithmetic progressions.

Throughout, *shell* means the reduced denominator $s = n/\gcd(k,n)$; a *cell* is a pair (n,k); and all reported statistics are finite-count observations over $1 \leq n \leq N$ for the stated N. These are empirical descriptions supported by proof where marked, not asymptotic theorems.

2 The shell numerator formula

We first give the closed form of a numerator inside a fixed shell. This is the structural seatbelt.

Lemma 1 (Fixed-shell numerator progressions)**.** *Let $s \geq 1$. In shell s, write $n = sm$ and $k = mt$, where $1 \leq t \leq s$ and $\gcd(t, s) = 1$. Then the reduced numerator of $a(n, k)$ is*

$$R_s(m, t) = s^2 m - s + t.$$

Consequently, for fixed s, the prime-numerator question is a union of $\varphi(s)$ arithmetic progressions modulo s^2:

$$R_s(m, t) \equiv t - s \pmod{s^2}, \qquad \gcd(t - s,\, s^2) = 1.$$

Proof. A cell (n, k) lies in shell s iff $n/\gcd(k, n) = s$, i.e. $\gcd(k, n) = n/s = m$, so $n = sm$ and $k = mt$ with $\gcd(t, s) = 1$ and $1 \leq t \leq s$. Using $\gcd(n(n-1) + k, n) = \gcd(k, n) = m$, the reduced numerator is

$$\frac{n(n-1) + k}{m} = \frac{sm(sm-1) + mt}{m} = s(sm-1) + t = s^2 m - s + t.$$

Reducing mod s^2 gives $R_s(m, t) \equiv t - s$. Since $\gcd(t, s) = 1$, $\gcd(t - s, s) = \gcd(t, s) = 1$, hence $\gcd(t - s, s^2) = 1$. As t ranges over the $\varphi(s)$ reduced residues mod s, we obtain $\varphi(s)$ residue classes mod s^2, each coprime to s^2. □

Proposition 1 (No within-shell numerator duplicates)**.** *For fixed shell s, a numerator value $R_s(m, t)$ occurs at most once.*

Proof. If $R_s(m, t) = R_s(m', t')$ then $s^2(m - m') = t' - t$. Since $1 \leq t, t' \leq s$, we have $|t' - t| < s \leq s^2$; the only multiple of s^2 in this range is 0, so $t = t'$ and hence $m = m'$. □

Proposition 1 has a useful role in the controls of §4: the recurrence of a prime value across the grid (its multiplicity, on average about 1.43 over the ranges computed) is entirely a *cross-shell* phenomenon — a prime value can recur in several *different* shells, but never twice in the *same* shell. Per-shell prime density is therefore not inflated by duplicates.

Remark 1 (Sample size per shell). The number of cells in shell s up to resolution N is $|S_N(s)| = \varphi(s)\lfloor N/s \rfloor$, since m ranges over $1 \leq m \leq \lfloor N/s \rfloor$ and t over the $\varphi(s)$ reduced residues mod s. This varies strongly across shells and is accounted for in §4.

Remark 2 (The map the demonstration exposes). The interactive renderer of §7 exposes the full per-cell map

$$(n, k) \;\mapsto\; (g, s, m, t) \;\mapsto\; R_s(m, t) \;\mapsto\; R_s(m, t) \bmod s^2 \;\mapsto\; \{\text{prime/composite}\},$$

while simultaneously displaying the shell-level comparison $\rho_N(s)/\widehat{\rho}_N(s)$. Figure 1 shows this ladder for a single cell; seeing a cell travel it — reduction, shell coordinates, numerator, residue class, primality, density contribution — is the bridge from the picture to the arithmetic.

3 Per-shell prime density and the predictor

Define the per-shell prime density

$$\rho_N(s) = \frac{\#\{(m, t) \in S_N(s) : R_s(m, t) \text{ is prime}\}}{|S_N(s)|}, \qquad S_N(s) = \{(m, t) : 1 \leq m \leq \lfloor N/s \rfloor,\ 1 \leq t \leq s,\ \gcd(t, s) = 1\}.$$

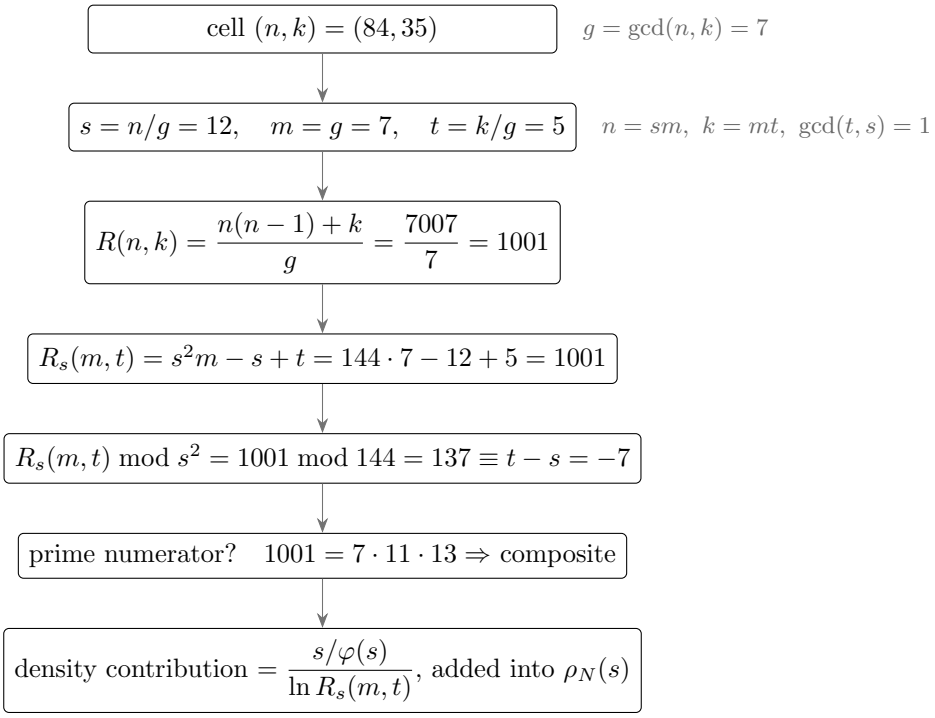

Figure 1: Formula ladder for one cell. A point (n,k) reduces by $g = \gcd(n,k)$ to shell coordinates $s = n/g$, $m = g$, $t = k/g$. Its reduced numerator becomes $R_s(m,t) = s^2 m - s + t$, lying in the admissible residue class $t - s \pmod{s^2}$. Prime cells contribute to $\rho_N(s)$, compared against the cellwise PNT-in-progressions predictor $\widehat{\rho}_N(s)$.

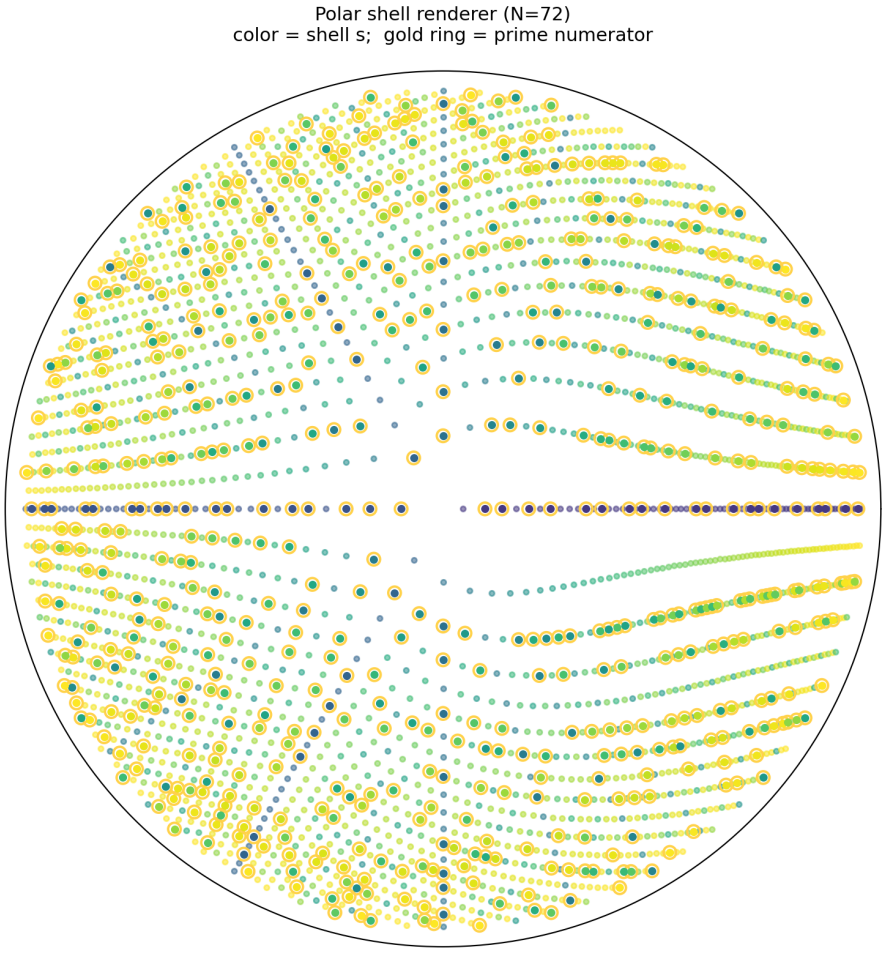

Figure 2: Polar shell renderer for the triangular-fractional grid. Chamber n is placed at radius $\sqrt{n}$, cell k at angle $2\pi k/n$, and color records the reduced-denominator shell $s = n/\gcd(k,n)$. Highlighted cells (gold ring) have prime reduced numerators $R_s(m,t) = s^2m - s + t$. This rendering is a visualization of the shell stratification; it is *not* the one-turn square-spiral coordinatization of the radial companion paper.

The size-blind comparison fails. A first, naive model compares $\rho_N(s)$ to the coprimality factor $1/\varphi(s)$. Over the computed ranges the ratio $\rho_N(s)/(1/\varphi(s))$ climbs strongly and monotonically with s (Spearman $\rho_{\mathrm{Sp}} \approx 0.96$–$0.99$, persistent across N; see §4). Taken alone this looks like a shell-dependent effect on primes.

The correct model is prime-in-progressions. By Lemma 1 the numerators in shell s are $\varphi(s)$ arithmetic progressions modulo s^2, each with common difference coprime to s^2. The prime-number theorem in arithmetic progressions gives a prime density near a value X with coprimality normalization $s^2/\varphi(s^2)$; because $\varphi(s^2) = s\varphi(s)$ this is exactly $s^2/(s\varphi(s)) = s/\varphi(s)$.

Definition 1 (PNT-in-progressions predictor)**.** *For $N \geq 1$ and $(m,t) \in S_N(s)$ set $R_s(m,t) = s^2 m - s + t$. Define*

$$\widehat{\rho}_N(s) = \frac{1}{|S_N(s)|} \sum_{\substack{1 \leq m \leq \lfloor N/s \rfloor \\ 1 \leq t \leq s,\ \gcd(t,s)=1}} \frac{s}{\varphi(s)\,\log R_s(m,t)}.$$

The coprimality factor $s/\varphi(s)$ is exact because $\varphi(s^2) = s\varphi(s)$; the prime-density term $1/\log R_s(m,t)$ is the usual asymptotic prime-number-theorem approximation. Thus the predictor is not fitted, but its prime-density component remains an asymptotic model. Writing the corrected ratio $Q_N(s) = \rho_N(s)/\widehat{\rho}_N(s)$, the climb seen against $1/\varphi(s)$ is absorbed: $Q_N(s)$ is flat, with no trend in s, and improves as N grows (Figure 3).

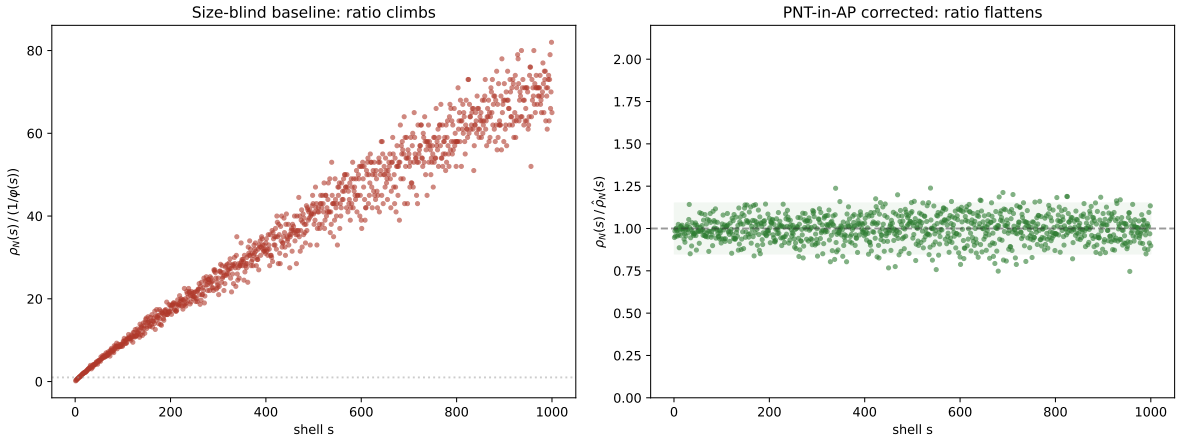

Figure 3: The shell climb is a baseline artifact. Left: against the size-blind $1/\varphi(s)$ comparison, the ratio climbs strongly with shell s. Right: against the cellwise PNT-in-progressions predictor $\widehat{\rho}_N(s)$, which includes the exact $s/\varphi(s)$ coprimality factor and the cellwise $1/\log R_s(m,t)$ size term, the ratio $Q_N(s)$ flattens around 1 (shaded band ± 0.15). $N = 1000$.

4 Controls

We record four controls; together they establish that the corrected fit is at the sampling-noise floor.

(a) Duplicates. By Proposition 1 there are no within-shell duplicate numerators, so $\rho_N(s)$ counts distinct primes; the ~ 1.43 global multiplicity is cross-shell. Verified: within-shell duplicate ratio 1.000, CV 0.000, across all shells tested.

(b) N-scaling. The corrected ratio is flat at every resolution and converges:

N	ρ_{Sp} (vs $1/\varphi$)	ρ_{Sp} (corr.)	CV (blind)	CV (corr., wtd)	shells
250	+0.959	+0.002	0.593	0.138	153
500	+0.979	−0.022	0.546	0.094	479
1000	+0.984	+0.040	0.539	0.076	1000
2000	+0.991	+0.024	0.541	0.058	2000

The size-blind trend is strong and stable (so the correction does real work, not fitting noise); the corrected trend is null at every N and its CV shrinks monotonically with N — the signature of a correct model, not a coincidental fit (Figure 4). CV is reported both unweighted and weighted by $|S_N(s)|$; the two agree closely.

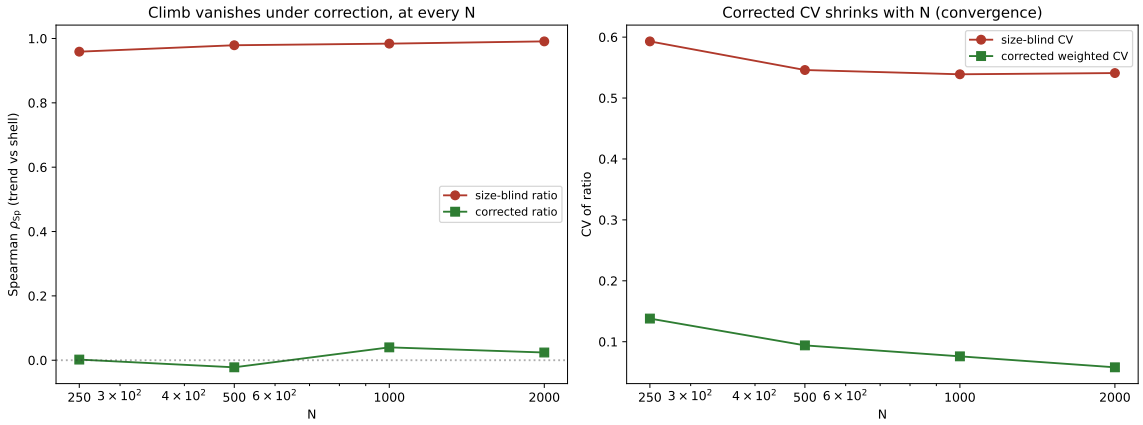

Figure 4: Robustness under resolution N. Left: the size-blind trend remains strong as N grows, while the corrected trend stays near zero. Right: the corrected coefficient of variation shrinks with N, consistent with convergence to the PNT-in-progressions baseline rather than a fitted one-window accident.

(c) Binomial sampling floor. At $N = 1000$, writing $\mathrm{SE}_s \approx \sqrt{\widehat{\rho}_N(s)(1-\widehat{\rho}_N(s))/|S_N(s)|}$, a fraction 0.994 of shells (994 of 1000) satisfy $|\rho_N(s) - \widehat{\rho}_N(s)| \le 2\,\mathrm{SE}_s$. The predictor matches the observed density to within two binomial standard errors almost everywhere; the residual is at the sampling floor.

(d) Shell-existence. Shell s exists in chamber n exactly when $s \mid n$, i.e. $n = sm$. The predictor $\widehat{\rho}_N(s)$ averages only over the cells that actually exist ($m = 1, \ldots, \lfloor N/s \rfloor$), so the divisibility condition is built into the parameterization and is not an additional sampling bias. (A note on small shells: the $1/\log R_s(m,t)$ model is weakest at very small numerators; small-s terms are included above and are visibly finite-size, and excluding $R_s(m,t) < e^2$ does not change the qualitative conclusion.)

5 Interpretation: where the action is

The edge is a boundary term, not a prime anomaly. Higher shells reach larger numerators ($R_s(m,t) \sim s^2 m$), so their prime density is lower through the size factor $1/\log R_s(m,t)$. What

looks, in the size-blind comparison, like "action concentrating at the high-shell edge" is exactly the size/boundary term — the same face → edge → corner discrepancy hierarchy recorded for the Cartesian shells in the Jordan Chamber Lift companion. The edge carries the deviation because that is where the boundary term lives, for primes or for any counted quantity.

Two entry frames. The same fact reads as intuitive or counterintuitive depending on the direction of approach. Entering *primes-first* — expecting primes to do something distinctive — makes the high-shell concentration a surprise. Entering *geometry-first* — knowing boundary terms concentrate at the edge — makes it the default. The governing frame here is geometry-first: the shell geometry determines *where* the deviation sits (the edge/size term), the arithmetic determines *what* is prime, and the lens makes both visible at once.

6 What is and is not claimed

Claimed. A triangular-fractional-native stratification of prime numerators by reduced-denominator shell, not found in the surveyed literature as a named object, with a controlled demonstration that per-shell prime density is well predicted by the prime-in-progression baseline (mod s^2, coprimality factor $s/\varphi(s)$) once numerator size is accounted for. The within-shell uniqueness (Prop. 1) is proven.

Not claimed. No new prime law (primes obey PNT in progressions on the lens; the novelty is the stratification and its clean demonstration). No Riemann-hypothesis relevance (inherited nonclaim). The two densities stay distinct: prime density here tracks the arithmetic progression density $(s/\varphi(s) \times 1/\log R_s(m,t))$, not the finite coprimality shell density $J_d(q)/q^d$ nor the visible-lattice density $1/\zeta(d)$. No higher-dimensional claim: a spiral/shell construction in three dimensions is deferred. Geometry is a lens, not a generator: the radial coordinate renders the structure, it does not create the prime pattern.

Classical context (cited, not fused). The grid is triangular-fractional and its Cartesian lift cubic; the classical triangular–cube identity is Nicomachus's theorem $(n(n+1)/2)^2 = \sum_{k\le n} k^3$. This is the classical neighborhood only: the n^3 there (a sum of cubes over n) is a different decomposition from the Jordan volume identity $\sum_{q|n} J_3(q) = n^3$ (a sum over divisors), a shared symbol rather than a shared mechanism. Euler's sine-product route to $\zeta(2) = \pi^2/6$ (already in the Jordan companion and the parent collar identity) is the analytic neighbor. No connection to Fermat's Last Theorem or power-sum equations is asserted; shared exponents are not a shared mechanism.

7 An interactive demonstration

The result is naturally displayed rather than only tabulated. A companion interactive artifact — a *polar shell renderer* (Figure 2) — lays out the fractional sequence radially, colors each cell by its shell, and highlights the **prime numerators**, which are the subject. Crucially it exposes the full per-cell map of Remark 2: clicking a cell reveals its reduction (g, s, m, t), its numerator $R_s(m,t) = s^2m - s + t$, its residue class $t - s \pmod{s^2}$, its primality, and its density contribution $\frac{s/\varphi(s)}{\log R_s(m,t)}$. A control varying N lets the viewer watch the distribution develop; a size-blind ↔ size-corrected toggle exhibits the entire "lens, not law" conclusion in a single switch. The demonstration is a visualization and reproducibility aid; the mathematical content is §§2–4.

Reproducibility

All statistics use a gcd-based enumeration (no totient sieve for counts) and a single prime sieve up to N^2; the numerator in shell s is computed directly as $R_s(m,t) = s^2m - s + t$ (Lemma 1). The N-scaling table, the binomial-floor check, and the size-blind-vs-corrected comparison are reproduced by an accompanying notebook.

References (to be completed in house style)

- J. Huckstead, *Divisor-Band Bijections and Totient Shells in the Triangular-Fractional Grid*, Zenodo, DOI 10.5281/zenodo.20533247.
- J. Huckstead, *The Jordan Chamber Lift: Denominator-Shell Collapse in Higher Dimensions*, 2026.
- Prime-number theorem in arithmetic progressions (Dirichlet; de la Vallée Poussin). Jordan totient and $\sum_{q|n} J_d(q) = n^d$: T. M. Apostol, *Introduction to Analytic Number Theory*, Springer 1976. Nicomachus's theorem. Ford circles (Ford 1938); Farey spacing statistics (Boca–Cobeli–Zaharescu 2000); visible-lattice density (Nymann 1972).